

Nonperturbative bound on high multiplicity cross sections in ϕ_3^4 from lattice simulation

Y.-Y.Charn^{*}

*Institute of Physics, Academia Sinica
Taipei, Taiwan 115, Republic of China*

R.S.Willey[†]

*Department of Physics,
University of Pittsburgh
Pittsburgh, PA 15260*

(Dated: November 7, 2018)

Abstract

We have looked for evidence of large cross sections at large multiplicities in weakly coupled scalar field theory in three dimensions. We use spectral function sum rules to derive bounds on total cross sections where the sum can be expressed in terms of a quantity which can be measured by Monte Carlo simulation in Euclidean space. We find that high multiplicity cross sections remain small for energies and multiplicities for which large effects had been suggested.

^{*}charng@phys.sinica.edu.tw, charng@phyast.pitt.edu

[†]willey@pitt.edu

I.

INTRODUCTION

In 1990, Ringwald [1] and Espinosa [2] presented a calculation of possible instanton induced baryon number violation accompanied by enhanced production of a large number of Higgs and W,Z bosons at high energy($E \sim n m/g$, where n is the number of outgoing particles of mass m , and g is a coupling constant of the theory). This has called attention to a more general and profound problem of quantum field theory. The problem is: for a given renormalized quantum field theory with weak renormalized coupling constant, what is the nature of the multiparticle production in that theory.

It has long been known that the perturbation-theory expansion in a theory with weak coupling can fail in high orders because of the factorial growth of the coefficients in the series [3]. So this problem can not be solved perturbatively because the perturbation series diverges rapidly at high order. In fact, independent of the instanton calculations, Goldberg [4], Cornwall[5] and, later Voloshin[6], Argyres, Kleiss, and Papadopoulos [7],and Brown[8] pointed out that in ϕ^4 scalar field theory the contributions of just the tree graphs to the multiparticle production amplitudes gives the $k!g^k$ behavior.

These complete tree graph calculations lead to a dramatic exponential growth of the rates for few \rightarrow many processes as the total energy E and number of final particles n increase together, and E exceeds some critical value of order $E \geq nm/g$. Something must turn this exponential growth off as it saturates unitarity bounds, but the phenomenological consequences could still be spectacular. Or perhaps the tree graph calculation is simply misleading - the dramatic exponential turn on only occurs for values of $n \sim 1/g$ for which the perturbation series diverges. Perhaps the answer is given just by taking the first few (small) terms of an asymptotic perturbation series with a small coupling constant. On the other extreme, A number of semiclassical calculations have suggested that these high multiplicity events are exponentially suppressed. [9]

It was found by Mawhinney and Willey [10] that a nonperturbative approach could be made through Monte Carlo simulation on a lattice. It was shown that using the analytic continuation from Euclidean lattice theory to Minkowski space quantum field theory, one could turn spectral function sum rules into an upper bound on inclusive multiparticle production. The program was carried through for ϕ^4 theory in $1 + 1$ dimension because,as

explained below, large lattices are required, and we only had the computing power for large two-dimensional (256^2) lattices. No signal for significant highmultiplicity processes was seen. However, the $1 + 1$ dimensional theory is a very special case in field theory.(no angular momentum, no concentration of radial wave function at spatial origin,..),so it is of interest to know the results for the $2 + 1$ dimensional theory. The tree diagram considerations which suggest large $1 \rightarrow n$ amplitudes in ϕ^4 are mainly combinatoric, and hold as well in three dimensions, as in two (or four). Furthermore, the ϕ^4 theory is superrenormalizable in three dimensions as well as in two. This is an essential element of the analysis presented below. (In four dimensions one has to deal with the presumed triviality of the theory and a cutoff. In less than four dimensions, the existence of the theory as the analytic continuation of the continuum limit of the Euclidean lattice theory is established. [11, 12].)

To deal with large three dimensional lattices we built a Beowulf parallel supercomputer with sixteen CPUs. We also used a Message Passing Interface(MPI) function call to parallelize our simulation program. We are able to achieve overall 7.4 Gflops at High Performance Computing Linpack Benchmark(HPL). The theoretical peak performance for sixteen CPUs is 12 Gflops. Compared with a 16 Gflops CRAY C90 at 16 CPUs, our parallel cluster has much better price/performance ratio. (For details of the construction and performance of this Beowulf computer, [13]).

II.

SPECTRAL FUNCTION SUM RULES AND BOUND ON HIGH MULTIPLICITY PRODUCTION PROCESSES

We start with some standard definitions to set the notation and display the ingredients used in the analysis below. In d spacetime dimensions, the canonical (unrenormalized) scalar field satisfies canonical commutation rules

$$[\dot{\phi}(x), \phi(0)]_{x_0=0} = -i\delta^{d-1}(\vec{x}) \quad (1)$$

The Wightman two-point function and its spectral decomposition are

$$\langle 0|\phi(x)\phi(0)|0\rangle = \int d\kappa^2 \rho(\kappa^2) \Delta^{(+)}(x; \kappa^2) \quad (2)$$

$$\Delta^{(+)}(x; m^2) = \int (dq) e^{-iqx} \Theta(q_0) 2\pi \delta(q^2 - m^2) \quad (3)$$

$$\left(dq = \frac{d^d q}{(2\pi)^d} \right) \quad (4)$$

$$2\pi\rho(p^2) = \int (d^d x) e^{ipx} \langle 0 | \phi(x) \phi(0) | 0 \rangle \quad (5)$$

$$= (2\pi)^d \sum_n \delta^{(d)}(p - p_n) \langle 0 | \phi(0) | n \rangle \langle n | \phi(0) | 0 \rangle \quad (6)$$

The states $|n\rangle$ are members of a complete set of in-,or out- states, and are labeled as $|q_1, \dots, q_n\rangle$ with

$$p_n^\mu = \sum_{a=1}^n q_a^\mu, \quad \omega_{(a)} = \sqrt{\vec{q}_{(a)}^2 + m^2} \quad (7)$$

The boldface sum over n implicitly includes some relativistic kinematical factors relating it to the relativistic invariant phase space integration.

$$\sum_n |n\rangle \langle n| = |0\rangle \langle 0| + \sum_{n=1}^{\infty} \frac{1}{n!} \prod_{a=1}^n \left(\int \frac{d^{d-1} q_{(a)}}{(2\pi)^{d-1} 2\omega_{(a)}} \right) |q_1 \dots q_n\rangle \langle q_1 \dots q_n| \quad (8)$$

Relativistic invariant phase space is simply related to this

$$(2\pi)^d \delta^d(p - p_n) \frac{1}{n!} \prod_{a=2}^n \left(\int \frac{d^{d-1} q_{(a)}}{(2\pi)^{d-1} 2\omega_{(a)}} \right) = \int d\Phi_n(E) \quad (9)$$

where E is the total cm energy $E = \sum_{a=1}^n q_{(a)}^0$

Separate out the single particle contribution to the spectral function.

$$\rho(p^2) = Z\delta(p^2 - m^2) + \hat{\rho}(p^2) \quad (10)$$

and

$$\langle q | \phi(0) | 0 \rangle = \sqrt{Z} \quad (11)$$

The CCR (1) imply the sum rule

$$1 = \int d\kappa^2 \rho(\kappa^2) \quad (12)$$

The integral is convergent in less than four space-time dimensions. Together with the positivity of the spectral function (6), these equations imply

$$0 \leq Z \leq 1 \quad (13)$$

For free field, $Z = 1$, and the field connects vacuum to single particle state only.

The renormalized field $\phi'(x)$ is defined by the normalization condition

$$\langle q | \phi'(0) | 0 \rangle = 1 \quad (14)$$

Thus $\phi(x) = \sqrt{Z}\phi'(x)$.

For the multiparticle states (6), it is an exercise with the LSZ reduction formulas to obtain

$$\langle q_1 \dots q_n | \phi(0) | 0 \rangle = \frac{1}{Z^{n/2}} G_F(p_n^2) Z^n \underline{\mathcal{I}}_{n+1}(q_1 \dots q_n) \quad (15)$$

Here $\tau_{n+1}(q_1 \dots q_n)$ is the Fourier transform of the vacuum expectation value of the T-product of $n+1$ ϕ fields, with the energy-momentum conserving delta function left off. The underline indicates that the external lines are all amputated ($q_1 \dots q_n$ are all on-shell.) G_F is the complete unrenormalized time-ordered two-point function.

The renormalization of all these quantities is

$$\rho = Z\rho', \quad G_F = ZG'_F, \quad \underline{\mathcal{I}}_{(n+1)} = \left(\frac{1}{Z^{\frac{n+1}{2}}} \right) \underline{\mathcal{T}}'_{(n+1)} \quad (16)$$

Then (6) becomes

$$2\pi\rho'_{(n)} = \int d\Phi_n(E) |G'_F(p_n^2)|^2 |\underline{\mathcal{T}}'_{(n+1)}(q_1 \dots q_n)|^2 \quad (17)$$

The G'_F depends only on the total four-momentum p_n (E in the c.m.) which is fixed in the n particle phase space integral, so it can be divided out. Divide also by particle density factor $2E$

$$\frac{\pi}{E} \frac{\rho'_{(n)}(p_n^2)}{|G'_F(p_n^2)|^2} = \frac{1}{2E} \int d\Phi_n(E) |\underline{\mathcal{T}}'_{(n+1)}(q_1 \dots q_n)|^2 = \Gamma_{(n)}(E) \quad (18)$$

which is the decay rate for one variable mass (E) ϕ particle to decay into n on-shell ϕ particles. The totally inclusive rate is

$$\Gamma(E) = \sum_n \Gamma_{(n)}(E) \quad (19)$$

One can think of the single timelike ϕ particle as formed by the annihilation of an $f\bar{f}$ pair, coupled weakly to the ϕ field. Then up to trivial kinematic factors, this is the analog of the QCD ratio R of hadron production to $\mu^+\mu^-$ production in e^+e^- annihilation. We do not write a slash for Γ . There is no reason to introduce a bare rate, so we simply write Γ with no slash for the physical quantity.

We now relate this rate to the inverse ϕ two-point function. (This has a simple diagrammatic representation. The probability for one timelike ϕ particle to go to many on-shell ϕ particles is given by the Cutkosky rules applied to the cuts of the ϕ self-energy diagrams). The spectral representation of the Feynman function follows from (2)

$$G_F(p^2) = \frac{Z}{p^2 - m^2} + \int d\kappa^2 \frac{\hat{\rho}(\kappa^2)}{p^2 - \kappa^2 + i\epsilon} \quad (20)$$

The imaginary part is

$$\Im G_F(p^2) = -\pi\hat{\rho}(p^2) \quad (21)$$

The imaginary part of G_F^{-1} is

$$\Im G_F^{-1}(p^2) = -\frac{-\Im G_F(p^2)}{|G_F(p^2)|^2} = \frac{\pi\hat{\rho}(p^2)}{|G_F(p^2)|^2} = \frac{E}{Z}\Gamma(E) \quad (22)$$

From all the information about G_F , we can write a dispersion integral for G_F^{-1} [14]

$$G_F^{-1}(p^2) = (p^2 - m^2)\left(1 + \int d\kappa^2 \frac{\gamma(\kappa^2)}{(\kappa^2 - m^2)(\kappa^2 - p^2 - i\epsilon)}\right) \quad (23)$$

with

$$\Im G_F^{-1}(p^2) = \pi\gamma(p^2) = \frac{E}{Z}\Gamma(E), \quad (p^2 = E^2) \quad (24)$$

We note that all of the properties of G_F enumerated so far are consistent with the possible existence of zeros of G_F on the real axis. If G_F has no additional poles, only one zero is possible, on the real axis in the gap between the pole and the start of the continuum. In any case, one can show that if such zero(s) of G_F exist, positivity of the spectral function is sufficient to show that the bound derived below is only strengthened [13]

The analytic continuation of the two-point function is immediate

$$p^0 \rightarrow ip_4, \quad p_M^2 = -p_E^2, \quad G_F(p_M^2) = -G_E(p_E^2) \quad (25)$$

$$G_E^{-1}(p^2) = (p^2 + m^2)\left(1 + \int d\kappa^2 \frac{\gamma(\kappa^2)}{(\kappa^2 - m^2)(\kappa^2 + p^2)}\right) \quad (26)$$

In this and subsequent equations in this section p^2 is Euclidean p_E^2 . The desired sum rules are now obtained by expanding both sides of this equation in powers of p^2 and equating the coefficients. The expansion of the left hand side defines the quantities Z', m'^2

$$G_E^{-1}(p^2) = \frac{1}{Z'}(m'^2 + p^2 + \dots) \quad (27)$$

while the right hand side is

$$G_E^{-1}(p^2) = m^2\left(1 + \int d\kappa^2 \frac{\gamma(\kappa^2)}{(\kappa^2 - m^2)\kappa^2}\right) + p^2\left(1 + \int d\kappa^2 \frac{\gamma(\kappa^2)}{\kappa^4}\right) + \dots \quad (28)$$

Matching coefficients of p^2 gives

$$\frac{1}{Z'} = 1 + \int d\kappa^2 \frac{\gamma(\kappa^2)}{\kappa^4} = 1 + \frac{1}{\pi Z} \int d\kappa^2 \frac{\kappa\Gamma(\kappa^2)}{\kappa^4} = 1 + \frac{2}{\pi Z} \int dE \frac{\Gamma(E)}{E^2} \quad (29)$$

Finally

$$\frac{2}{\pi} \int dE \frac{\Gamma(E)}{E^2} = Z \left(\frac{1}{Z'} - 1 \right) \leq \frac{1}{Z'} - 1 \quad (30)$$

If the probability for production of high multiplicity states of c.m. energy E turns on exponentially at some critical energy E_* , the integral of $\Gamma(E)/E^2$ will turn on exponentially as the range of integration over E extends beyond E_* . But by above, this integral is bounded by $\frac{1}{Z'} - 1$, which can be extrapolated from lattice MC calculation of the slope of the inverse of the Fourier Transform of the two-point correlation.

III.

CRITICAL ENERGY AND LATTICE MOMENTA

According to the papers cited in the introduction, there may exist a critical energy E_* ($\sim n m/g$) at which the probability for production of high multiplicity final states suddenly begins exponential growth. We require an estimate of that critical energy and its relation to the momentum of the lattice propagator. Repeat the spectral representation for $G_E(p^2)$ (p^2 is the Euclidean momentum squared).

$$G_E(p^2) = \frac{Z}{p^2 + m^2} + \int d\kappa^2 \frac{\hat{\rho}(\kappa^2)}{p^2 + \kappa^2} \quad (31)$$

κ^2 is the square of the c.m. energy of the state $|n\rangle$ contributing to the spectral function $\hat{\rho}$ (section two). For large p^2 , the (convergent) integral is dominated by $\kappa^2 \leq p^2$. Then for the integral to be sensitive to dramatic behavior for $\kappa^2 \approx E_*^2$ requires $p^2 \geq E_*^2$. But the relevant p is the Euclidean lattice momentum which lies in the Brillouin zone $-\pi/2 \leq p_\mu \leq \pi/2$, or (lattice) $p^2 \leq d(\pi/a)^2$. Combining these observations leads to the desideratum

$$d \left(\frac{\pi}{a} \right)^2 > E_*^2 \quad (32)$$

Take the square root and divide by mass m

$$E_*/m < \sqrt{d}\pi\xi_L \quad (33)$$

where $1/ma = \xi_L$ is the correlation length in lattice units.

The estimation of E_* for the tree diagrams of ϕ^4 in three plus one dimensions has been refined in the papers cited in the introduction. We have adapted these calculations to two plus one dimensions and find [13]

$$\frac{E_*}{m} = 74\pi \frac{m}{\lambda} \quad (34)$$

Substituting this result into (33) we obtain

$$74\pi\frac{m}{\lambda} < \sqrt{d}\pi\xi_L \quad (35)$$

There is also a pair of general conditions for extrapolating results obtained from a calculation on a lattice to results in continuum limit: The correlation length should be much greater than the lattice spacing and much less than the linear lattice size. Thus

$$1 \ll \frac{74}{\sqrt{3}}\frac{m}{\lambda} < \xi_L \ll N \quad (36)$$

Note that for fixed $\frac{\lambda}{m}$ of order one, these conditions can all be satisfied by a large enough lattice (N of order one or two hundred).

IV.

LATTICE SIMULATION AND CONTINUUM LIMIT

The Monte Carlo simulation for the scalar field on the lattice is standard. The physical field, masses, and coupling constant are dimensionful quantities. When put on a lattice the lattice spacing a can be scaled out and the dimensionless action written in terms of dimensionless lattice fields and mass and coupling constant. The distinction becomes important in taking the continuum limit. In three (Euclidean) dimensions the scalings are

$$\phi = \frac{1}{\sqrt{a}}\phi_L, \quad \mu_0^2 = \frac{1}{a^2}\mu_{0L}^2, \quad \lambda = \frac{1}{a}\lambda_L \quad (37)$$

The lattice action is

$$S = \sum_{\vec{n}} \left\{ \frac{1}{2} \sum_{\nu} [\phi_L(\vec{n} + \vec{e}_{(\nu)}) - \phi_L(\vec{n})]^2 + \frac{1}{2}\mu_{0L}^2 \phi_L(\vec{n})^2 + \frac{1}{4}\lambda_L \phi_L(\vec{n})^4 \right\} \quad (38)$$

We start with a standard Metropolis update algorithm, and with each sweep of the lattice measure the expectation of ϕ and the two-point correlation. (For this discussion of the lattice calculation all quantities are in lattice units. We suppress the subscript L until we come back to the continuum limit). We take the lattice Fourier transform of ϕ and compute the output lattice propagator

$$G(k) = \langle \phi(k)\phi(-k) \rangle \quad (39)$$

and plot the inverse of this against the inverse of the free lattice propagator

$$G_0^{-1}(k) = \hat{k}^2 + m^2 \quad (40)$$

with

$$\hat{k}^2 = 4 \sum_{\nu} \sin^2(k_{\nu}/2) \quad (41)$$

This is the inverse of the massless free lattice propagator.

Z' and m' are obtained from the plot of $G^{-1}(\hat{k}^2)$ against the inverse of the free massless lattice propagator.(27)

As we approach the continuum limit we are also approaching the critical line fig (3), and the simple Metropolis update begins to suffer critical slowing down. As one approaches the critical line, both the correlation length and autocorrelation time diverge. The relation of the correlation length ξ and autocorrelation time τ is[15, 21]

$$\tau \sim \xi^z \sim L^d \quad (42)$$

where z is the dynamic exponent and τ is measured in number of sweeps. In a system of finite size, the correlation length never really diverges. Cutting it off at the size of the lattice, the autocorrelation time increases as the lattice size increases as

$$\tau \sim L^z \quad (43)$$

when close to critical. Depending on the value of z , one can require a large amount of CPU time to generate a fixed number of independent data as one approaches critical on large lattices. For straight Metropolis update, z is close to two. See Table I.

To overcome the critical slowing down, one must define appropriate nonlocal (or collective) variables and a new dynamics for driving them. Progress has been made with some nonlocal algorithms for both discrete spin models and continuum fields. Swendsen and Wang[16] have used the Fortuin-Kastelyn [17] percolation map for the Potts model to define collective coordinates that allow domains to be inverted with zero free energy cost. Some modifications were proposed by Wolff[18]

The algorithm for the ϕ^4 field theory is a little more complicated. Brower and Tamayo[20] proposed an algorithm for ϕ^4 field theory based on the Swendsen and Wang algorithm. Here we will follow Brower and Tamayo's method but switch to the Wolff algorithm. Table I compares the dynamic exponent values for the Ising model in different dimensions with different algorithms. One can see that the Wolff algorithm is more effective than the Swendsen and Wang algorithm in three dimension.

TABLE I: Comparison of the values of the dynamic exponent z for different algorithms for Ising model in various dimensions[22].

dimension d	Metropolis	Wolff	Swendsen-Wang
2	2.167 ± 0.001	0.25 ± 0.01	0.25 ± 0.01
3	2.02 ± 0.02	0.33 ± 0.01	0.54 ± 0.02
4	-	0.25 ± 0.01	0.86 ± 0.02

In our simulation, the update algorithm consists of two parts:(**1**) a conventional Metropolis Monte Carlo update for the $\phi(x)$ field and (**2**) Wolff cluster identification and flipping. Identification of a cluster of ϕ field, requires introduction of a discrete variable $s_{\vec{n}}$

$$\phi(\vec{n}) = s_{\vec{n}}|\phi(\vec{n})| \quad (44)$$

where $s_{\vec{n}} = \pm 1$.

For details of the cluster algorithm see [13] Here we only present some illustration of its effectiveness and correctness.In fig(1) we show plots of autocorrelation in measurements of $\langle\phi\rangle$ for one set of input parameters, with and without the cluster algorithm. We see an improvement by a factor of roughly 200 in the number of sweeps required to reach e^{-1} fall off.

There is a price to be paid for this improvement in generation of uncorrelated equilibrium configurations. That is in the actual measurement of $\langle\phi\rangle$ itself. With only Metropolis update, on large lattices, there are very many sweeps between tunneling, and measurement of $\langle\phi\rangle$ is trivial. The cluster update changes sign of $\langle\phi\rangle$ frequently and it is harder to dig out its infinite volume (no tunneling) limit.

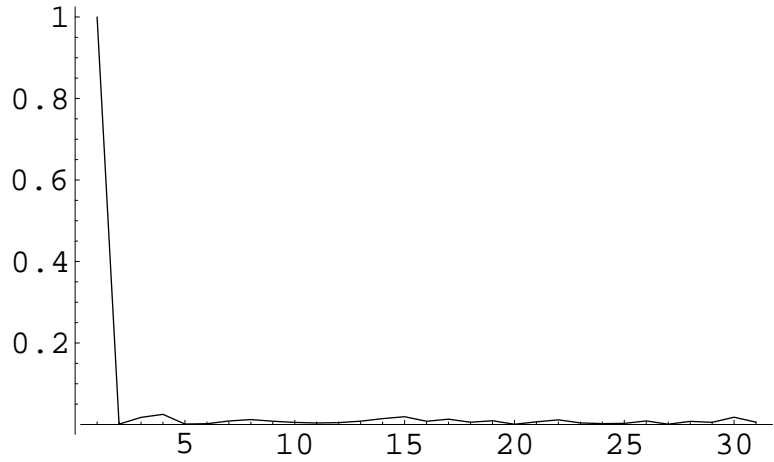
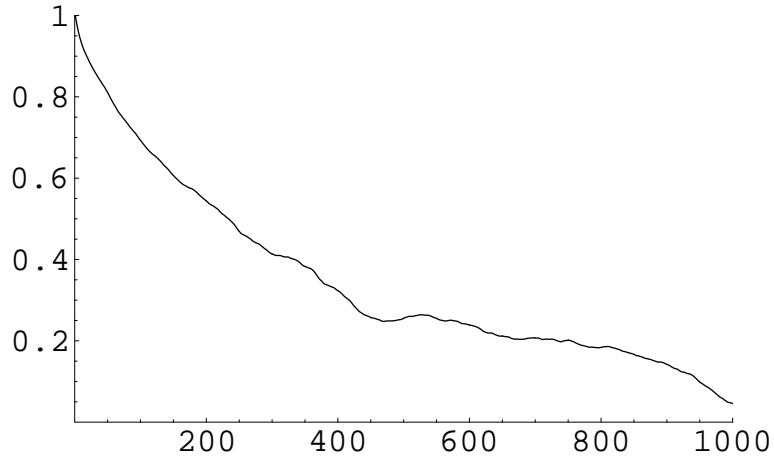


FIG. 1: The autocorrelation for the $\langle\phi\rangle$ with and without the cluster update algorithm. The e^{-1} point for the one without the cluster update algorithm is at about 400(top). The autocorrelation length for the one with cluster update algorithm is about 2 only(bottom).

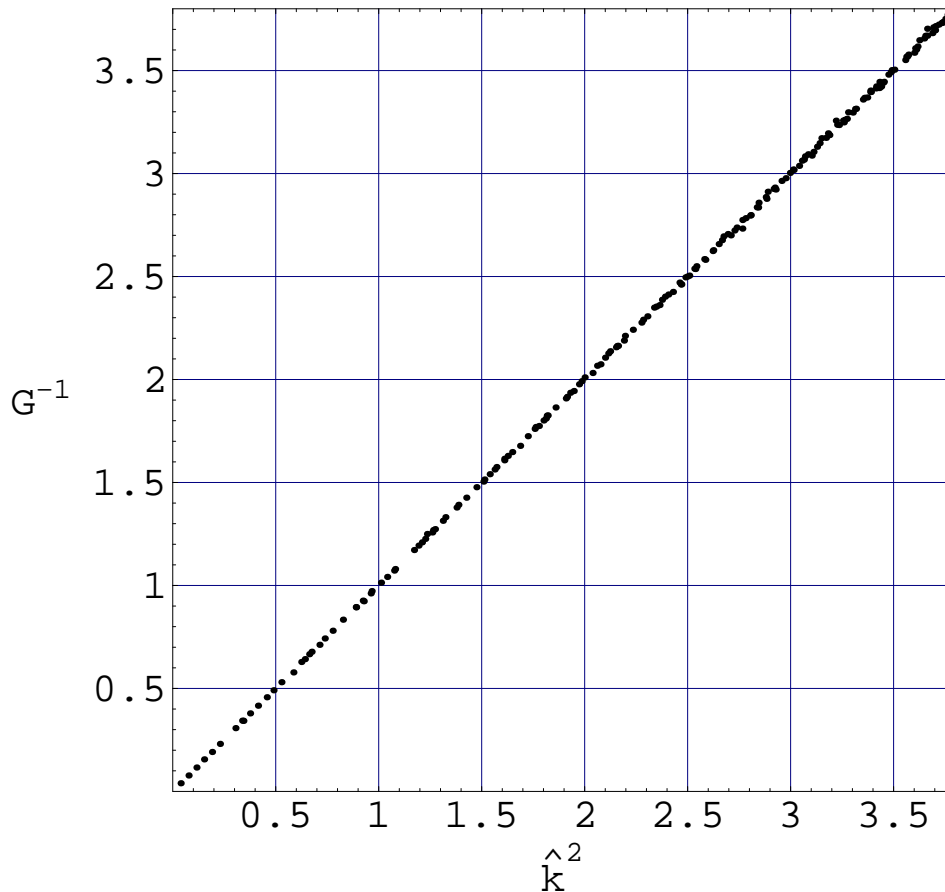


FIG. 2: Result of Monte Carlo evaluation of $G^{-1}(k)$ for $\lambda = 0, \mu_0^2 = 0.001$ plotted against exact analytic massless propagator $\hat{k}^2 = 4 \sum_{\nu} \sin^2(k_{\nu}/2)$ on a 32^3 lattice. Error bars on Monte Carlo results are too small to show up on this plot.

An important check is to do the MC simulation for the coupling constant λ equal to zero. For this case we know the exact analytic (free field) solution. In particular, m'^2 is equal to input bare mass squared (necessarily positive) and $Z' = Z = 1$). This is shown in fig2 where G^{-1} from the simulation (with $\lambda = 0$) is plotted against the free massless inverse propagator (\hat{k}^2). The result is a straight line of unit slope, offset by the mass squared (0.001 and not visible in this example).

Although the physics is entirely dependent on $\lambda \neq 0$, for the MC simulation program and the program for analysis of the MC data, zero is just one possible value of λ . So the above result does check a substantial part of the simulation and data analysis programs.

For $\lambda \neq 0$, we have also, for a few sets of input parameters, paid the price in longer CPU time required when the cluster algorithm is turned off, and checked that the results $(m', 1/Z')$ are the same, within small statistical errors, with or without the cluster algorithm.

We will return to another test, the Ising limit, after our discussion of the phase structure and the continuum limit.

There are both general theoretical and heuristic and practical considerations involved in extracting real world results from the Euclidean lattice results. The general theoretical underpinning comes from the program of constructive field theory which has provided the results that for $d < 4$, the ϕ_d^4 Quantum Field Theory can be obtained as the analytic continuation of the Euclidean ϕ_d^4 field theory, which in turn may be obtained as the continuum limit of a lattice ϕ_d^4 theory. This program is described in detail in two long and mathematical monographs [11],[12]. A simple example is again provided by the free theory ($\lambda = 0$) which is completely determined by the two-point function. When the lattice propagator (41) is rewritten in terms of physical dimensionful quantities with the lattice spacing a inserted where required to give the propagator its correct physical dimension, the limit $a \rightarrow 0$ is simply seen to be the free Euclidean propagator. However, in the general case, the output from the MC simulation is numerical, and the limit has to be done by extrapolation. To see what is involved, we consider the phase diagram fig (3).

The ϕ^4 theory on a lattice of lattice spacing a has two dimensionless parameters, μ_{0L}^2, λ_L (37). Since λ is finite and μ_0^2 is only linearly divergent ($\sim 1/a$), both of these dimensionless parameters go to zero in the limit $a \rightarrow 0$. Thus the point at the origin in fig(3) corresponds to the Euclidean field theory. So start on dimensionless lattice (N^3) at some point in μ_{0L}^2, λ_L plane. Choice of parameters is subject to requirement that output $\xi'_L = 1/m'_L$ satisfy

$$1 \ll \xi'_L \ll N \tag{45}$$

This is an obvious condition for lattice spacing and volume effects to be small. To proceed toward the origin, go to lattice $N_2 = 2N$, and adjust input μ_{0L}^2, λ_L to get output $\xi'_{L_2} = 2\xi'_L$. This corresponds to keeping same physical volume and correlation length while reducing lattice spacing to half of starting value. A sequence of these steps corresponds to one of the dashed lines in fig(3). Note that at each step ξ'_L is increasing (doubling) so the first inequality in (45) is increasingly better satisfied (The second remains the same).

The ϕ^4 field theory ($a \rightarrow 0$) is specified by a single finite dimensionless constant, which we

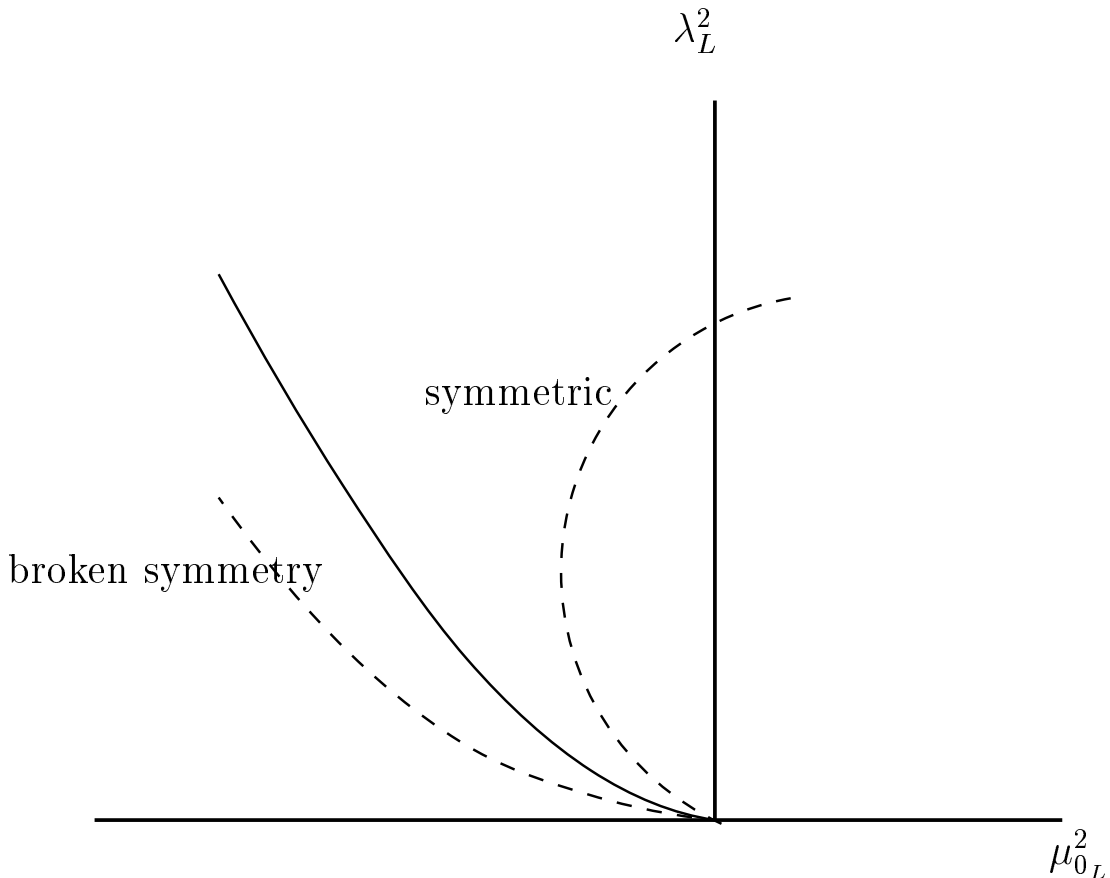


FIG. 3: The phase diagram for the three-dimensional, single component scalar ϕ^4 theory. The solid line separates the symmetric phase from the broken symmetry phase. The dashed lines are lines of constant physics.

may take to be λ/m' ; so “constant physics” is implemented by fixed value of λ/m' . Also, the two other finite dimensionless quantities we can measure, $1/Z'$, and $\langle\phi\rangle/\sqrt{m'}$, are functions of λ/m' in the limit of $a \rightarrow 0$. As the origin is approached along one of the dashed lines, the values of these quantities should approach their continuum values. In practice, When the change in values in successive steps is less than the estimated error, we accept those values.

We briefly discuss the relation of this work to the Ising model of Statistical Mechanics. This is in itself of some interest, and it also provides another check of our MC simulations. The EFT limit is reached by following one of the dashed lines into the origin ($\lambda_L \rightarrow 0$). The Ising model limit is approached by following a dashed line (in broken symmetry phase) out to infinity ($\lambda_L \rightarrow \infty$). The Euclidean lattice Lagrangian (38) can be rewritten as

TABLE II: The Monte Carlo simulation of $32^3 \phi_3^4$ theory at Ising limit ($\lambda \rightarrow \infty$). The table shows the critical temperature β_c at different λ values.

λ	μ_{0c}^2	$-\frac{\mu_{0c}^2}{\lambda}$	β_c
100	-31	.31	.25
300	-75	.25	.23
1000	-228	.228	.222

$$\mathcal{L} = - \sum_{\langle \vec{i}, \vec{j} \rangle} \phi(\vec{i}) \phi(\vec{j}) + \sum_{\vec{i}} \frac{\lambda}{4} \left(\phi^2(\vec{i}) - \frac{-\mu_0^2 + 2d}{\lambda} \right)^2 \quad (46)$$

All quantities here are in lattice units (subscript L suppressed). The sum over angle bracket is standard notation for sum over nearest neighbors, each pair counted once. An irrelevant constant has been added. Compare with the Hamiltonian of Ising model

$$\mathcal{H} = -\beta \sum_{\langle \vec{i}, \vec{j} \rangle} \sigma_{\vec{i}} \sigma_{\vec{j}}, \quad (47)$$

The limit $\lambda \rightarrow \infty$ will exponentially suppress the second term in equation (46), and convert the continuous field variable to a spin variable.

$$\lim_{\lambda \rightarrow \infty} \phi(\vec{i}) = \pm \sqrt{\frac{-\mu_0^2 + 2d}{\lambda}} \equiv \sqrt{\beta} \sigma_{\vec{i}} \quad (48)$$

with $\sigma_{\vec{i}} = \pm 1$ and

$$\beta = \frac{-\mu_0^2 + 2d}{\lambda} \quad (49)$$

To compare with the Ising limit, we do the simulation with the $\lambda \gg 1$ and calculate the VEV $\langle \phi \rangle$ for different μ_0^2 . We start in the symmetric phase with one λ value and vary the value of μ_0^2 until the VEV is no longer zero. In our simulation, when $\lambda \gg 1$, we get a very sharp transition from the symmetric phase to broken symmetry phase. So, it is very easy to identify the critical μ_{0c}^2 . Table II shows the β_c from the simulation at 32^3 with different λ . The third row shows that when $\lambda = 1000$, the β_c from our simulation with a continuous field variable is very close to the (numerically) known value 0.2217... for the 3d Ising Model. This gives us additional confidence in our MC simulation.

V.

ANALYSIS AND RESULTS

A fortran program implementing the Metropolis and cluster update algorithms described above provides the equilibrium lattice configurations i.e. the sets of values $\phi(\vec{n})_t$ for t from 1 to N_t where t denotes the t 'th sweep through the lattice and N_t is the number of sweeps through the lattice after thermalization. For large lattices with N_t less than the time before tunneling, and the cluster update turned off, the vev is

$$\langle \phi \rangle = 1/N_t 1/N^3 \sum_1^{N_t} \sum_{\vec{n}} \phi(\vec{n})_t \quad (50)$$

When the cluster update is turned on, the sign of the vev as defined above changes frequently and $\langle \phi \rangle$ is very small, even deep in the broken symmetry phase. So the vev is then defined as

$$\langle |\phi| \rangle = 1/N_t 1/N^3 \sum_1^{N_t} \left| \sum_{\vec{n}} \phi(\vec{n})_t \right| \quad (51)$$

The program also does the lattice Fourier transform of ϕ and constructs the k-space lattice propagator. This output is then input for a Mathematica program which determines m'^2/Z' and $1/Z'$ from fit of output lattice propagator

$$G(\hat{k}^2)^{-1} = (1/Z')(m'^2 + \hat{k}^2 + \dots) \quad (52)$$

The estimated errors associated with $1/Z'$ and m' for fixed lattice (N) are statistical, originating from the Monte Carlo, and systematic from extrapolation to k equal to zero in the fit. (We can not use the data point $k = 0$ because it contains a volume singularity) The results are collected in Table III

We can see in the Table the implementation of the approach to the continuum limit by a sequence of steps in which the physical correlation length (physical mass) is kept fixed while the linear number of lattice points (N) and the correlation length in lattice units (ξ'_L) are both doubled. The ratio N/ξ'_L (L/ξ) is kept fixed (~ 5.6). We also see that λ/m' keeps the same value within expected errors through these steps as do the dimensionless quantities, $1/Z'$, $\langle \phi \rangle / \sqrt{m}$, consistent with their being functions of λ/m' only. This suggests that these values are insensitive to lattice artifacts and approaching the continuum limit. This is illustrated in figures (4),(5), (6).

TABLE III: The results of fit to data from the simulations on different size lattices(N^3),the input parameters μ_{0L}^2, λ_L ,and the output dimensionless coupling parameter λ/m' ,and the output correlation length $\xi'_L = 1/m'_L$,the slope $1/Z'$, and the dimensionless ratio $\langle |\phi| \rangle / \sqrt{m'}$.

N^3	μ_{0L}^2	λ_L	$\frac{\lambda}{m'}$	ξ'_L	$\frac{1}{Z'}$	$\frac{\langle \phi_0 \rangle}{\sqrt{m'}}$
32^3	-0.161	0.2	1.13(2)	5.7(1)	1.008(2)	0.78(1)
64^3	-0.078	0.1	1.13(4)	11.3(4)	1.012(3)	0.80(2)
128^3	-0.0384	0.05	1.11(5)	22.11(1.0)	1.012(5)	0.80(2)
256^3	-0.01905	0.025	1.13(8)	45.4(3.0)	1.010(8)	0.79(3)

We also check the absence of finite volumn effects. We hold the input parameters, μ_{0L}^2, λ_L ,fixed and vary N. In Table IV we see that when the linear size of the lattice is greater than three times the output correlation length, the output quantities are unchanged under further increase in N. Note that in Table III the ratio of N to ξ'_L is kept fixed at 5.6 as one moves along a dashed curve in fig(3)

TABLE IV: The finite size effect with fixed input parameters $\mu_{0L}^2 = 0.01905, \lambda_L = 0.025$.

μ_{0L}^2	λ_L	N^3	ξ_L	$\frac{\lambda}{m'}$	$\frac{1}{Z'}$	$\frac{\langle \phi_0 \rangle}{\sqrt{m'}}$
-0.01905	0.025	64^3	41.5(6.5)	1.04(16)	1.002(3)	0.78(14)
-0.01905	0.025	128^3	45.1(3.8)	1.127(97)	1.0011(35)	0.77(10)
-0.01905	0.025	256^3	45.4(3.0)	1.13(8)	1.010(8)	0.795(97)

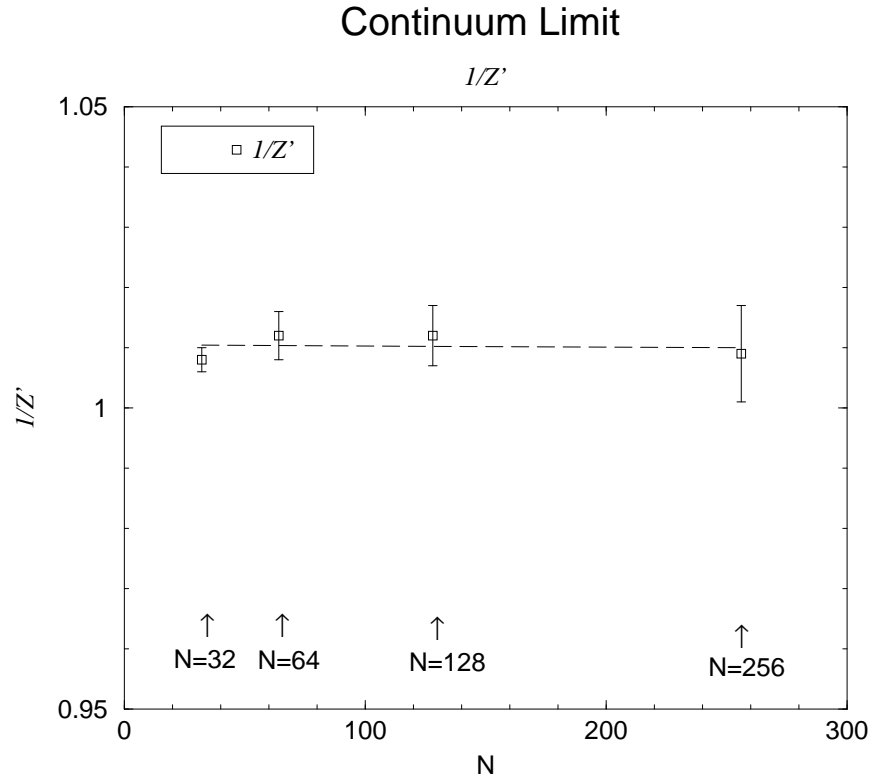


FIG. 4: Continuum limit for $\frac{1}{Z'}$. The plot shows the insensitivity to lattice spacing for $\frac{1}{Z'}$.

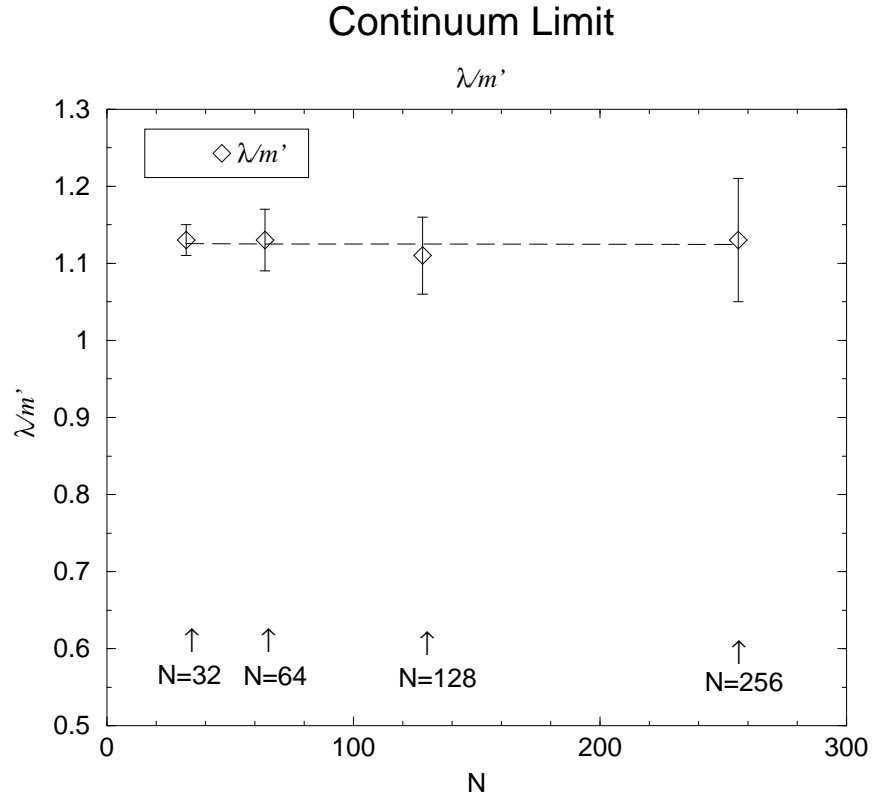


FIG. 5: Continuum limit for the $\frac{\lambda}{m'}$. The plot shows the insensitivity to lattice spacing for $\frac{\lambda}{m'}$.

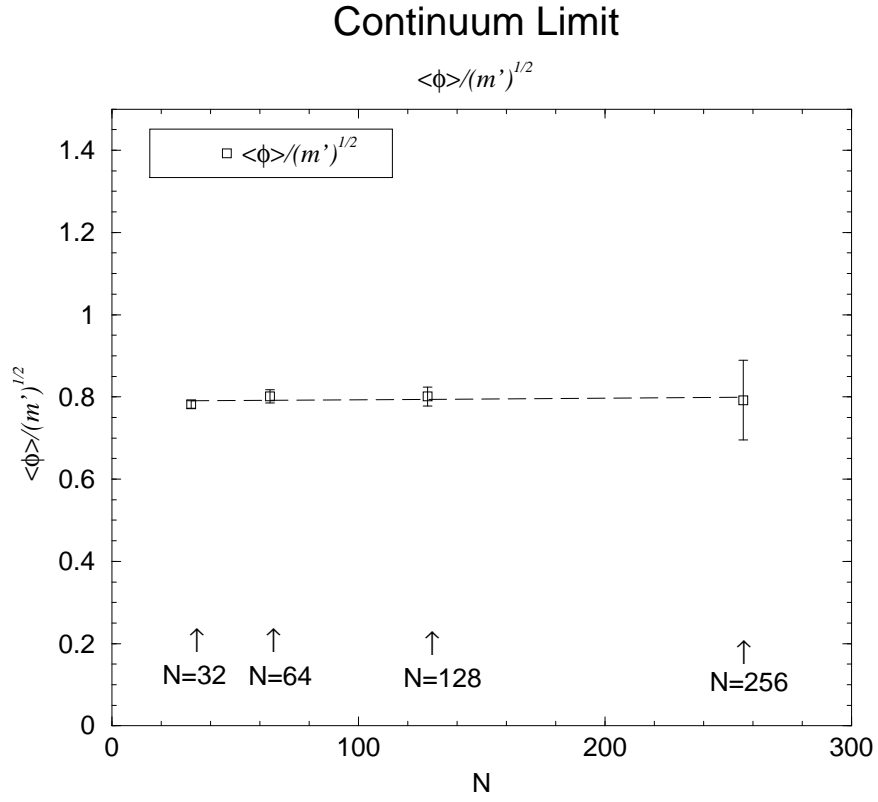


FIG. 6: Continuum limit for the $\frac{\langle \phi_0 \rangle}{\sqrt{m'}}$. The plot shows the insensitivity to lattice spacing for $\frac{\langle \phi_0 \rangle}{\sqrt{m'}}$.

The significance of these results is brought out in the qualitative behavior of the quantities in Table V.

TABLE V: Size of lattice and condition for appearance of high multiplicity inelastic processes

1	\ll	$\frac{74}{\sqrt{3}} \frac{m'}{\lambda}$	$<$	ξ_L	$<$	$< N$	$1/Z' - 1$
1		37.8		5.7		32	.008(2)
1		37.8		11.3		64	.012(3)
1		38.5		22.1		128	.012(5)
1		37.8		45.4		256	.010(8)

The condition (36),(45)

$$1 \ll \frac{74}{\sqrt{3}} \frac{m'}{\lambda} < \xi_L \ll N \quad (53)$$

is not satisfied for the first three lattices, but is clearly satisfied for the last (finest grained) lattice. And there is no significant change in the value of $1/Z' - 1$ in going from the first lattice to the last. We consider this to be strong nonperturbative evidence that there is no exponential turn on of high multiplicity production processes for energies greater than some critical energy of order $n \frac{m}{\lambda}$

Although the most significant feature of TableV is the absence of large *change* in $1/Z' - 1$ as one passes into a region of parameter space in which the divergence of perturbation theory suggests the possibility of exponential growth of high multiplicity processes; one can still ask: what would be a large value or a small value of $1/Z' - 1$ in this context? What is the significance of the single number 0.010 ? In the weak coupling regime, we can take low order perturbative effects to define small. We have calculated $1/Z' - 1$ through two-loop order, in broken symmetry phase. [13]. We have chosen to specify the constructed ϕ_3^4 theory by the output λ/m' . For the perturbation expansion parameter (g) we take $\frac{\lambda}{8\pi m'}$. The result is

$$\frac{1}{Z'} = 1 + \frac{\lambda}{8\pi m'}(3/4) + \left(\frac{\lambda}{8\pi m'}\right)^2(-1.83) + \dots \quad (54)$$

For our particular lattice MC solution, $\lambda/m' = 1.13$ ($g = .045$). This gives the perturbative value

$$1/Z' - 1 = .0337 - .0037 + \dots \simeq .030 \quad (55)$$

The lattice MC result from Table IV is .010(8), which is close to consistent with the perturbative estimate. So any nonperturbative contribution is of the same order as or smaller than the perturbative estimate, which is small.

We can still ask: If there were important high multiplicity processes contributing to (30), how would they show up in this analysis? From all the spectral equations in section II, we see that this would show up as Z substantially less than one. In this case, the last step in (30) leads to an inefficient bound. So we go back to

$$\frac{2}{\pi} \int dE \frac{\Gamma(E)}{E^2} = Z \left(\frac{1}{Z'} - 1 \right) \leq \frac{1}{Z'} - 1 \quad (56)$$

By manipulation of the equations of section II, one can show that $Z/Z' \leq 1$. Then on the righthand side of the equation

$$Z \left(\frac{1}{Z'} - 1 \right) = \frac{Z}{Z'} - Z \leq 1 - Z \leq 1 \quad (57)$$

So even if the decay were dominated by high multiplicity final states, the integral of the inclusive rate is bounded by one.

$$\frac{2}{\pi} \int dE \frac{\Gamma(E)}{E^2} \leq 1 \quad (58)$$

While in this limit we expect $1/Z'$ to be much greater than one i.e. $1/Z' - 1$ is a very inefficient bound in this case.

It is also interesting to compare the perturbative and nonperturbative calculations of $\langle |\phi| \rangle / \sqrt{m'}$. The perturbative expression is

$$\sqrt{\frac{m'}{2\lambda}} \left(1 + \frac{\lambda}{8\pi m'} (39/8) + \dots \right) \quad (59)$$

For $\lambda/m' = 1.13$ this is 0.81. The lattice MC value from TableIV is 0.795(95) (or rounding 0.80(1))

In conclusion: The absence of any significant change in the value of $1/Z' - 1$ from the lattice MC calculation as one moves from coarse grained to fine grained lattices, and that the value is close to the two-loop perturbative result, are strong evidence that there is no exponential enhancement of the rate for the high multiplicity processes $1 \rightarrow n$ for $n \simeq 1/g$. We are not sensitive to the presence or absence of exponential suppression of rates for asymptotic values of E, n , which by definition are very small and only effect terms far out in the series (54).

Acknowledgments

Y.Y.Chang is partially supported by the National Science Council of the Republic of China under the Grant No. of NSC-90- 2811- 001-071

- [1] A. Ringwald, Nucl. Phys. **B350**, 1(1990)
- [2] O. Espinosa, Nucl. Phys. **B343**,310(1990)
- [3] J. Zinn-Justin, Phys. Rep. **70**, 109(1981)
- [4] H. Goldberg, Phys. Lett. **B246**, 435(1990)
- [5] J.M. Cornwall, Phys. Lett. **B243**, 271(1990)
- [6] M.B. Voloshin, Phys. Lett. **B293**, 389(1992)
- [7] E.N. Argyres, R.M.P. Kleiss, and C.G. Papadopoulos, Nucl. Phys. **B341**, 42(1993),**B341**, 57(1993)
- [8] L.S. Brown, Phys. Rev. **D46**, R4125(1992)
- [9] V.A.Rubakov, hep-ph/9511236
- [10] R.D. Mawhinney and R.S. Willey, Phys. Rev. Lett. **74**, 3728.(1995)
- [11] J. Glimm and A. Jaffe, *Quantum Physics. A Functional Integral Point of View* (Springer-Verlag, New-York, 1987)
- [12] R. Fernández, Fröhlich and A. Sokal, *Random Walks, Critical Phenomena, and Triviality in Quantum Field Theory* (Springer-Verlag, New York, 1992)
- [13] Y.Y. Chang, **PhD** thesis, University of Pittsburgh, 2001. hep-lat/0110217.
- [14] J.Schwinger, Brandeis Summer Institute Lectures on Theoretical Physics (1959)
- [15] I. Montvay and G. Munster, *Quantum Fields on a Lattice* (Cambridge, United Kingdom 1994),
- [16] R.H. Swendsen and J.S. Wang, Phys. Rev. Lett. **58**, 86(1987)
- [17] C.M. Fortuin and P.W. Kasteleyn, Physica (Amsterdam) **57**, 536(1972).
- [18] U. Wolff, Phys. Rev. Lett. **62**, 361(1989)
- [19] D. Kandel, E. Domany, D. Ron, A. Brandt and E. Loh, Jr., Phys. Rev. Lett. **60**,1591(1988).
- [20] R.C. Brower and P. Tamayo, Phys. Rev. Lett. **62** 1087(1989)
- [21] P.C. Hoenberg and B. Halperin, Rev. Mod. Phys **49**, 435 (1977).
- [22] The values are taken from Coddington and Bailie(1992), Matz *et al.*(1994) and Nightingale

and Blote(1996). The dynamic exponent of Metropolis algorithm has not been measured in four dimensions.